metals

MDPI

Article

Composite Coating Prepared with Ferulic Acid to Improve the Corrosion Resistance and Blood Compatibility of Magnesium Alloy

Zhijin Han [1], Haojie Guo [1], Yifan Zhou [1,*], Liguo Wang [1], Kun Zhang [2] and Jing-an Li [1,*]

[1] School of Materials Science and Engineering, Henan Key Laboratory of Advanced Magnesium Alloys, Zhengzhou University, 100 Science Road, Zhengzhou 450001, China; hzj201912192012600@gs.zzu.edu.cn (Z.H.); 20212192013527@gs.zzu.edu.cn (H.G.); lgwang@zzu.edu.cn (L.W.)
[2] School of Life Science, Zhengzhou University, 100 Science Road, Zhengzhou 450001, China; zhangkun@zzu.edu.cn
* Correspondence: zhouyf@zzu.edu.cn (Y.Z.); lijingan@zzu.edu.cn (J.-a.L.)

Abstract: Magnesium (Mg) alloy has been used for medical vascular stents because of its good biocompatibility and degradability, but its rapid degradation and poor blood compatibility limits its further application. In this study, ferulic acid (FA) was conjugated onto the polydopamine (PDA) deposited Mg-Zn-Y-Nd alloy to prepare a PDA/FA multi-functional coating with better corrosion resistance and blood compatibility. The results suggest that the PDA/FA coating possessed potential application for surface modification of a medical Mg alloy.

Keywords: cardiovascular stent; Mg-Zn-Y-Nd alloy; blood compatibility; corrosion resistance; ferulic acid

check for updates

Citation: Han, Z.; Guo, H.; Zhou, Y.; Wang, L.; Zhang, K.; Li, J.-a. Composite Coating Prepared with Ferulic Acid to Improve the Corrosion Resistance and Blood Compatibility of Magnesium Alloy. *Metals* **2022**, *12*, 545. https://doi.org/10.3390/met12040545

Academic Editor: Sebastian Feliu Batlle

Received: 23 February 2022
Accepted: 21 March 2022
Published: 23 March 2022

Publisher's Note: MDPI stays neutral with regard to jurisdictional claims in published maps and institutional affiliations.

Copyright: © 2022 by the authors. Licensee MDPI, Basel, Switzerland. This article is an open access article distributed under the terms and conditions of the Creative Commons Attribution (CC BY) license (https://creativecommons.org/licenses/by/4.0/).

1. Introduction

Cardiovascular disease (CVD) remains a major cause of health loss for all regions of the world [1]. The most common treatment strategy for cardiovascular disease has been implantation of vascular stents [2]. Vascular stents are divided into drug-eluting stents (DES), bare metal stents (BMS), and degradable stents. Traditional metal vascular stents (such as cobalt chromium alloy and 316 L stainless steel) are undegradable and face the risk of secondary surgery. Drug-eluting stents are superior to conventional non-degradable scaffolds in reducing major adverse clinical events [3]. Although DES can significantly reduce the incidence of restenosis, it still has some disadvantages, such as late-stent thrombosis (LST), accelerated atherosclerosis, and delayed endothelialization. Anti-proliferative drugs (sirolimus, paclitaxel, etc.) inhibit endothelial cell proliferation [4–6]. The degradation of degradable polymer stents will produce local acidity, resulting in severe inflammation and intimal hyperplasia [7]. Therefore, the search for biodegradable metal stents has become a hot point in the field of vascular disease research [8].

Magnesium (Mg) alloy cardiovascular stents have attracted much attention because of their excellent properties, such as excellent biocompatibility and degradability [9–11]. However, the application of the Mg alloy in cardiovascular stents still faces some problems, such as rapid degradation rate, thrombosis, and insufficient endothelization. Consequently, it is necessary to reduce the corrosion rate, blood compatibility, and cell compatibility of Mg alloys by surface modification and the introduction of loaded drugs to prepare functional coatings. At present, surface-coating technology has been widely used in magnesium alloy, because it effectively decreases the degradation rate of the Mg alloy substrate and improves its biocompatibility. In addition, loading drugs into the coating can also obtain specific functions. Ferulic acid (FA) is the main effective component of Angelica sinensis, ferula, and other traditional Chinese medicines. It exists in fruits and vegetables such as corn and rice bran [12]. It has the physiological characteristics of being

anti-inflammatory, antibacterial, anti-virus, anti-aging, and anti-cancer [13,14]. In addition, it also has the function of anti-platelet aggregation. Its sodium salt has been used in the adjuvant treatment of coronary heart disease, atherosclerosis, and other diseases [15]. More importantly, studies have shown that FA can promote angiogenesis [16] and endothelial cell proliferation [17], and it can inhibit the proliferation of smooth muscle cells [18]. Zhang et al. found that FA can improve the blood compatibility of poly (3-hydroxybutyrateco-3-hydroxyhexanoate) (PHBHHx) membrane [19]. These characteristics show that FA is an ideal drug for cardiovascular stents. Polydopamine (PDA) has the characteristics of easy adhesion, easy preparation, and good biocompatibility, and it has a functional group amino, which can play the role of double-sided adhesive. However, it is difficult to be applied in practice due to poor blood compatibility. PDA is rich in functional groups such as amino groups [20–22]. Therefore, PDA can be selected to load FA [23]. The preparation of functional coatings by surface treatment is a common method by which to enhance the comprehensive properties of Mg alloys, such as anodic oxidation [8,24], fluorination [25], phosphate treatment [26], electro-grafting [27,28], silylation [29–31], and alkali heat treatment [19,20,32]. Among them, alkali heat treatment has the characteristics of having a simple method, being easy to prepare, having a low cost, and a degradable coating, which is convenient for the next coating preparation and conducive to cell adhesion [19]. To solve the lack of corrosion resistance of the Mg alloy, an alkaline thermal coating could be prepared under the PDA coating.

In this work, Mg-OH/PDA/FA composite coatings were successfully prepared on the Mg-Zn-Y-Nd alloy. The Mg-Zn-Y-Nd alloy was treated with alkali heat treatment, then modified with dopamine, and the PDA coating was obtained as the fixed layer. FA were grafted on PDA through carbodiimide chemistry and the Mannich reaction. It has been reported that FA is dose-dependent, i.e., different concentrations of phenolic hydroxyl and polyphenol hydroxyl will have different effects on the growth behavior of cells [33]. The PDA coating was treated with FA for three different time periods to conjugate different doses of FA.

2. Materials and Methods

2.1. Chemicals and Materials

The Mg-Zn-Y-Nd alloy (Mg-2.0Zn-0.46Y-0.5Nd, extruded) used as the basal material was obtained from Henan Key Laboratory of Advanced Magnesium Alloy (Zhengzhou, China). Dopamine hydrochloride and Trans-Ferulic acid were purchased from Aladdin Co., (Shanghai, China). N-(3-(dimethylamino) propyl)-N0-ethylcarbodiimide hydro-chloride (EDC), n-hydroxysuccinimide (NHS), and 2—(N-morpholine) ethanesulfonic acid (MES) were purchased from Shanghai Macklin Biochemical Co., Ltd. (Shanghai, China).

2.2. Preparation of PDA-FA Composite Coating on Mg-Zn-Y-Nd Alloy

The Mg-Zn-Y-Nd alloy substrates were polished and cleaned as reported previously [34]. Then, the Mg-Zn-Y-Nd alloy substrates were promptly soaked in 3 M NaOH solution for 8 h at 60 °C. The pretreated substrates were rinsed with deionized water (dH_2O) 3 times. The samples, after alkali treatment, were coded as Mg-OH. The treated substrates were then soaked in 2 mg/mL dopamine Tris buffer solution (pH 8.5) at 37 °C for 24 h to obtain a PDA coating, The PDA coating was rinsed 3 times with dH_2O and dried with hot air, and the samples were coded as PDA. Afterward, FA was immersed in a water-soluble carbodiimide (WSC) solution (pH 5.4) containing 1 mg/mL N-(3-dimethylaminopropyl)-N'-ethylcarbodiimide (EDC), 0.24 mg/mL nhydroxysuccinimide (NHS), and 2 mg/mL 2-(N-morpholino) ethanesulfonic acid hydrate (MES) for 30 min at 37 °C in order to activate the carboxyl group of ferulic acid. Then, the PDA samples were soaked in WSC solution at 37 °C for three different time gradients. The three times gradients of the activated FA carboxyl group reacting with the PDA amino group were coded as FA-1 h, FA-3 h and FA-6 h. The preparation process of Mg-OH/PDA/FA coating was shown in Figure 1.

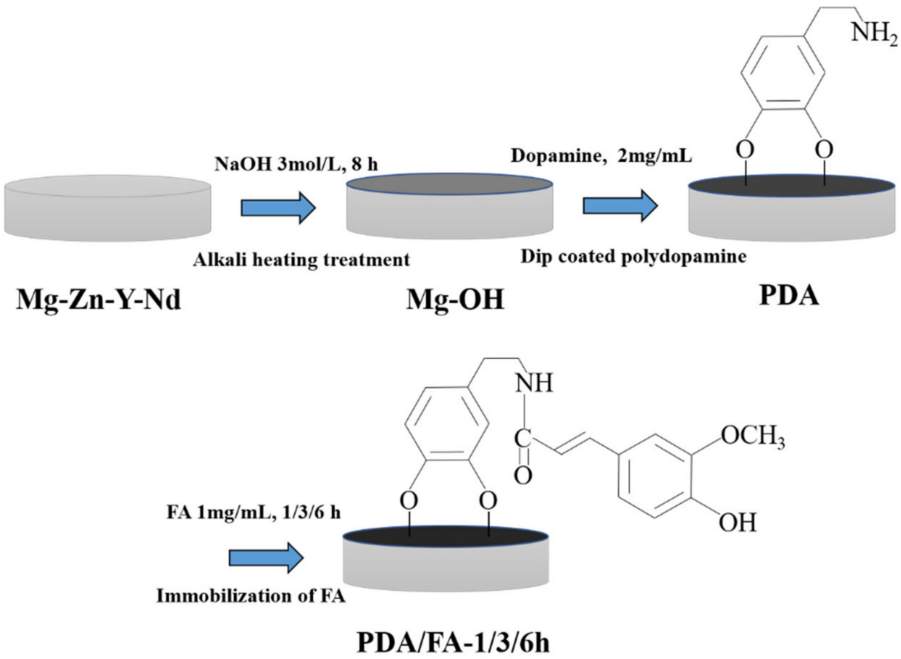

Figure 1. The scheme for preparing Mg-OH/PDA/FA composite coating.

2.3. Characterization of the Mg-OH/PDA/FA Composite Coating

The surface morphology of the Mg-Zn-Y-Nd, Mg-OH, PDA, FA-1 h, FA-3 h, FA-6 h samples was observed by scanning electron microscope (SEM, FEI Quanta200, Eindhoven, The Netherlands) [22]. The composition and functional groups of Mg-Zn-Y-Nd, Mg-OH, PDA, FA-1 h, FA-3 h, FA-6 h samples were analyzed by total reflection Fourier transform infrared spectroscopy (FTIR, Bruker VERTEX 70v, Karlsruhe, Germany) [35]. The water contact angle of Mg-Zn-Y-Nd, Mg-OH, PDA, FA-1 h, FA-3 h, FA-6 h samples was measured by water contact angle-measuring equipment (DSA 100, Krüss, GmbH, Hamburg, Germany) at room temperature, and then the average of six readings was calculated from each sample by DSA 1.8 software (Version 1.8, Krüss, GmbH, Hamburg, Germany) [36]. The micromorphology and roughness of Mg-Zn-Y-Nd, Mg-OH, PDA, FA-1 h, FA-3 h, and FA-6 h were measured by atomic force microscopy (AFM, Bruker/mnltimode, Billerica, MA, USA) [37]. The chemical composition was further studied by X-ray photoelectron spectroscopy (XPS, Axis Supra, Kyoto, Japan) [38]. Electrochemical corrosion tests including potential dynamic polarization (potentiodynamic polarization plots, scanning rate: 0.0005 v/s, 20 min) and electrochemical impedance spectroscopy (Nyquist EIS spectra, Zhengzhou Shi Ruisi Instrument Technology Co., Ltd., Zhengzhou, China) were carried out by RST5200f electrochemical workstation (Shiruisi, Zhengzhou, China) with a three-electrode system in simulated body fluid (SBF) solution [39].

2.4. Blood Compatibility Tests

2.4.1. Adhesion and Degeneration of Fibrinogen

The fibrinogen denaturation experiment was carried out by quantification of γ-chain exposure by using the ELISA method [40]. In short, fresh blood with heparin sodium as a anticoagulant was centrifuged at 3000× *g* rpm to acquire poor-platelet plasma (PPP). Then the sample to be tested was placed on a 24-well plate, and 50 µL PPP was added to each sample, after which it stood at 37 °C for 1 h. After washing with normal saline 3 times, HRP-labeled goat anti-human fibrinogen-binding antibody was added to each sample. Finally, the absorbance at 450 nm was measured by an enzyme-labeling instrument.

2.4.2. Platelet Adhesion Test

Fresh whole blood was taken from healthy volunteers. Sodium citrate was used as an anticoagulant, centrifuged at 1500× *g* r/min for 10 min, and the supernatant was absorbed to obtain platelet-rich plasma (PRP). After that, the samples were soaked in 50 µL PRP and incubated for 1 h at 37 °C. Finally, all samples were washed 3 times with normal saline for 3 min each time to clear non-adherent platelets, then fixed with 4% paraformaldehyde, and finally dehydrated and dried with 25, 50, 75, 90, and 100% ethanol solutions. The surface morphology was observed by SEM [41].

2.4.3. Hemolysis Test

Fresh blood and normal saline were mixed in the ratio of 4:5 to prepare diluted blood, and then the sample was immersed to be tested for 30 min in 37 °C normal saline. Then the diluted blood was added to 37 °C normal saline and ultrapure water for 1 h as a negative control group and a positive control group. Finally, the solution was sucked out and centrifuged at 2500× *g* rpm for 5 min. Finally, the absorbance at 545 nm wavelength was measured by an enzyme-labeling instrument. The hemolysis ratio (HR) is calculated as follows:

$$HR = \frac{OD_t - OD_n}{OD_p - OD_n} \times 100\%, \quad (1)$$

where OD_t represents the optical density value of the sample group, OD_n represents the optical density value of the negative control group, and OD_p represents the optical density value of the positive group. If the hemolysis rate exceeds 5%, it means that hemolysis reaction may occur [42]. Otherwise, it indicates that the material meets the requirements of medical materials.

2.5. DPPH Free Radical Content Test

The scavenging ability of free radicals of each sample was determined by the 2,2-diphenyl-1-pyridyl (DPPH) method and the DPPH free radical decolorization method from purple to yellow. That is, the sample was immersed in 2 mL DPPH ethanol solution (0.02 mmol/mL) and then treated in the dark at 37 °C for 1 h. Then, the absorbance at 517 nm was measured by enzyme plate absorbance meter (synergyh1, BioTek, Vermont, VT, USA).

2.6. Statistical Analysis

The results were indicated as mean ± standard deviation, and the difference was statistically significant if the $p < 0.05$.

3. Results and Discussion

3.1. Surface Characterization

Figure 2 shows the SEM morphology and surface element composition of each sample. After polishing, the surface of the Mg alloy is smooth. A dense and uniform $Mg(OH)_2$ passivation layer is formed after alkali heat treatment, and the O element appears in the coating. After depositing a PDA film, C and N elements appear in the coating, and regular cracks appear on the surface, which may be caused by the cracks of the alkaline thermal coating itself or the self-polymerization of dopamine. When FA was fixed for 1 h, some cracks were filled. At 3 h, the cracks were basically filled up, and some particles are generated. At 6 h, more detailed and irregular cracks were produced, which may be caused by the overreaction between FA and PDA. With the increase of fixed time, the content of the C element gradually increased and the content of the O element decreased.

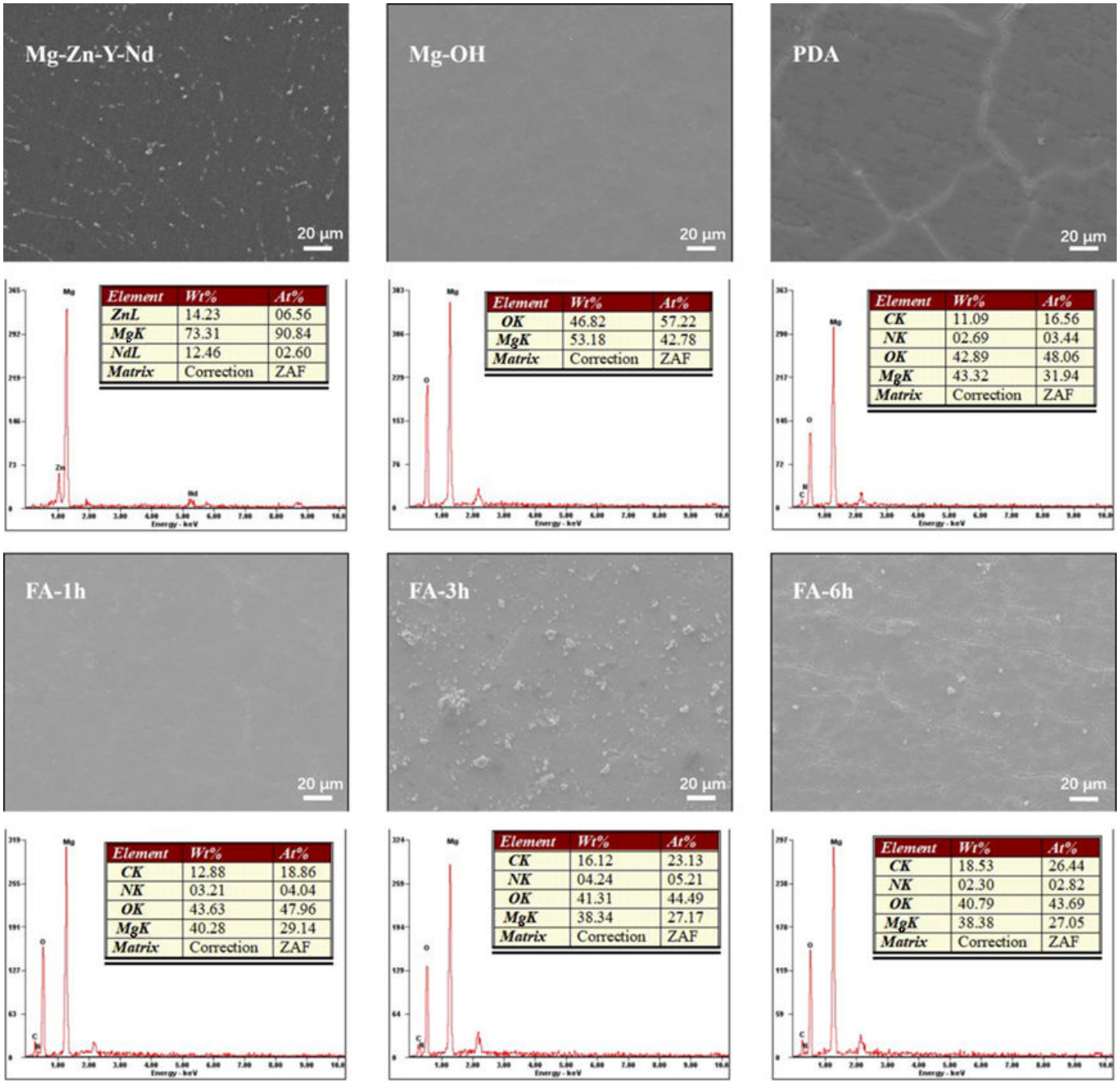

Figure 2. Surface SEM morphology and EDS spectrum of samples.

Here, the chemical composition and structure of PDA before and after FA fixation were analyzed by infrared technology and XPS technology, and the successful fixation of FA was verified. Figure 3 shows the infrared spectrum of the samples. Alkali heat treatment can introduce a large amount of—OH on the surface, so it has obvious infrared absorption of Mg-OH at 3704 cm^{-1}. After dipping in dopamine, the substrate presented several peaks at 1204.1099 cm^{-1}, which are characteristic peaks for stretching and bending vibrations of C-O, C-N of the PDA molecules on the material surface, respectively. Further modifications, in case of FA grafting, include the absorption band around 1300–800 cm^{-1} being reinforced. Three new peaks at 1671 cm^{-1}, 1530 cm^{-1}, and 1365 cm^{-1} were observed which are characteristic peaks for C=O stretching, N-H bending, and C-N stretching of the amide bond. This preliminarily confirmed the successful fixation of FA.

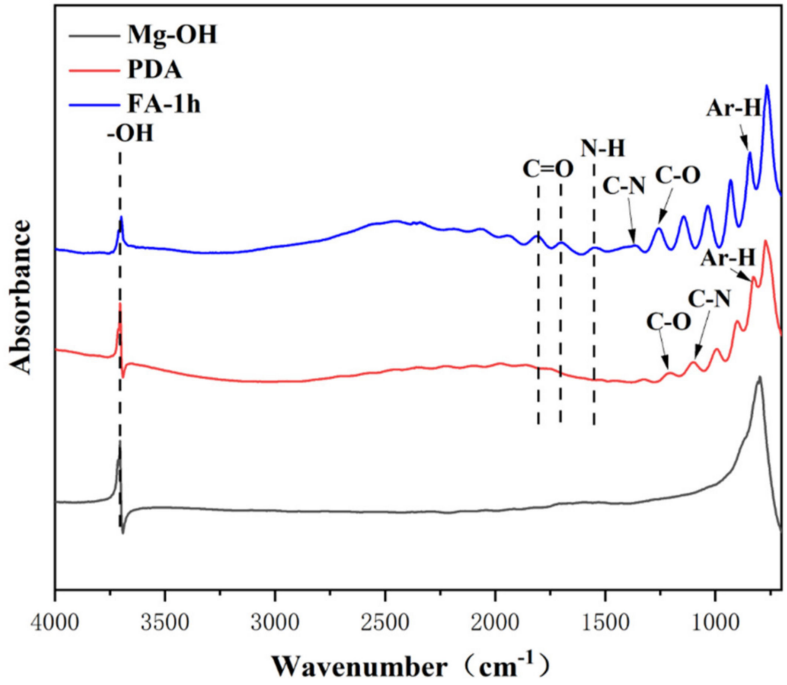

Figure 3. Infrared spectra of different samples.

As shown in Figure 4, the fixed FA will significantly reduce the N peak (399.5 eV) and O peak (531.5 eV) and increase the C peak (248.8 eV). In the C1s spectrum, 286 and 288.4 eV peaks were enhanced and ascribed to the increase of phenolic hydroxyl groups immobilized by FA and the formation of amide bonds. New peaks appeared at 400.4 and 531.5 eV in N1s and O1s, and the peaks moved toward high-binding energy, which is ascribed to the formation of amide bond-N-C=O.

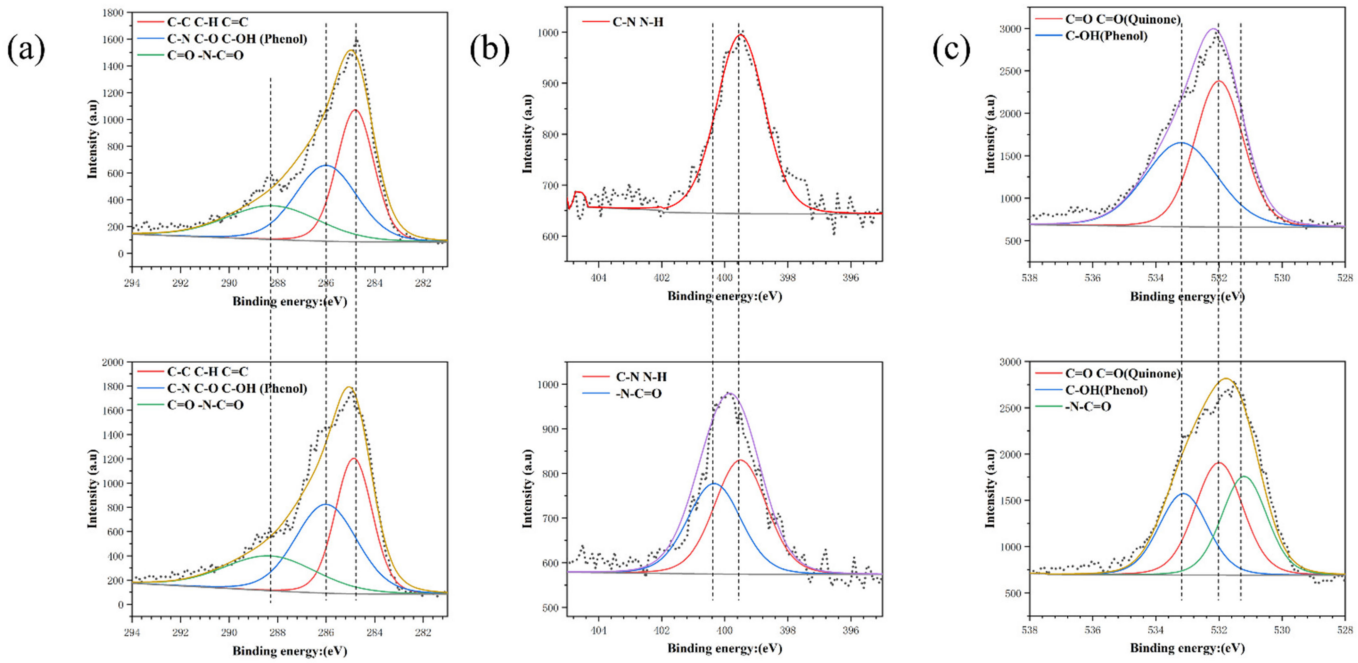

Figure 4. High resolution spectra of C1s (**a**) N1s (**b**) and O1s (**c**) of PDA and Fa-1 h.

As shown in Figure 5, the roughness values of the Mg alloy after polishing is small, only 7.44 nm. An $Mg(OH)_2$ passivation layer was formed after alkali heat treatment, and the roughness values increased to 30.8 nm. After dip coating with dopamine, the roughness

values continued to increase to 33.4 nm, which may be related to cracks and particles in the dopamine coating. However, after fixing FA, the roughness values increases to 35.9 nm, and with the increase of fixing time, the roughness values gradually decrease to 29.5 nm at 3 h and 26.7 nm at 6 h, which may be ascribed to FA filling the cracks of PDA coating.

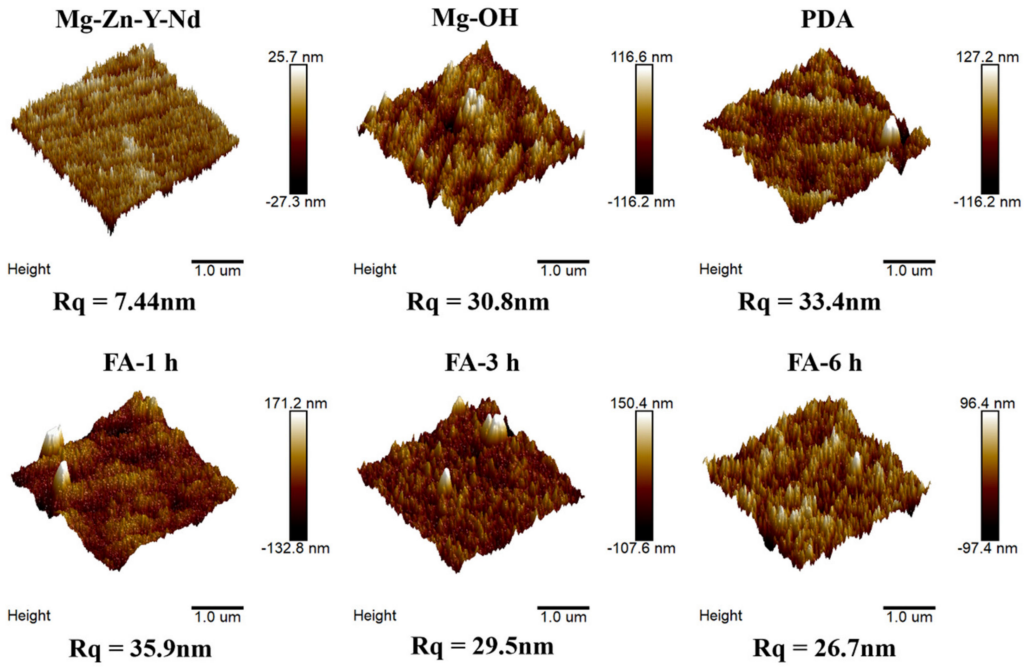

Figure 5. Atomic force topography and roughness of samples.

As shown in Figure 6, the Mg alloy had good hydrophilicity, and the water contact angle was only 28.3°, which may be due to low roughness and overpolishing. After alkali heat treatment, the water contact angle increased to 45.7°, which may be due to the formation of the $Mg(OH)_2$ passivation layer and the increase of roughness. After dip coating with dopamine, due to the addition of hydrophilic groups such as dopamine amino group and phenolic hydroxyl group, the water contact angle decreased significantly to 12°. With the increase of FA fixation time, the water contact angle gradually increased, which may be due to the addition of C=C hydrophobic groups. Although amide bonds were formed, the hydrophilicity was still slightly reduced, to 18.6°, 24.5°, and 37° respectively, but they were far less than 90°, showing hydrophilicity.

3.2. Corrosion Resistance Tests

As shown in Figure 7 and Table 1, the corrosion resistance of the Mg alloy was enhanced after the PDA/FA coating was prepared. The self-corrosion potential first increased and then decreased. After alkali heat treatment, the self-corrosion current decreased by two orders of magnitude compared with the Mg alloy. After dip-coating with dopamine, the self-corrosion current decreased by an order of magnitude compared with alkali heat treatment. After FA was fixed, the self-corrosion current first decreased and then increased with the increase of time. The variation law of the self-corrosion current was Fa-3 h > Fa-1 h > PDA > Mg-OH > Fa-6 h > Mg-Zn-Y-Nd. The variation law of the self-corrosion potential was Fa-3 h > Fa-1 h > PDA > Fa-6 h > Mg-OH > Mg-Zn-Y-Nd.

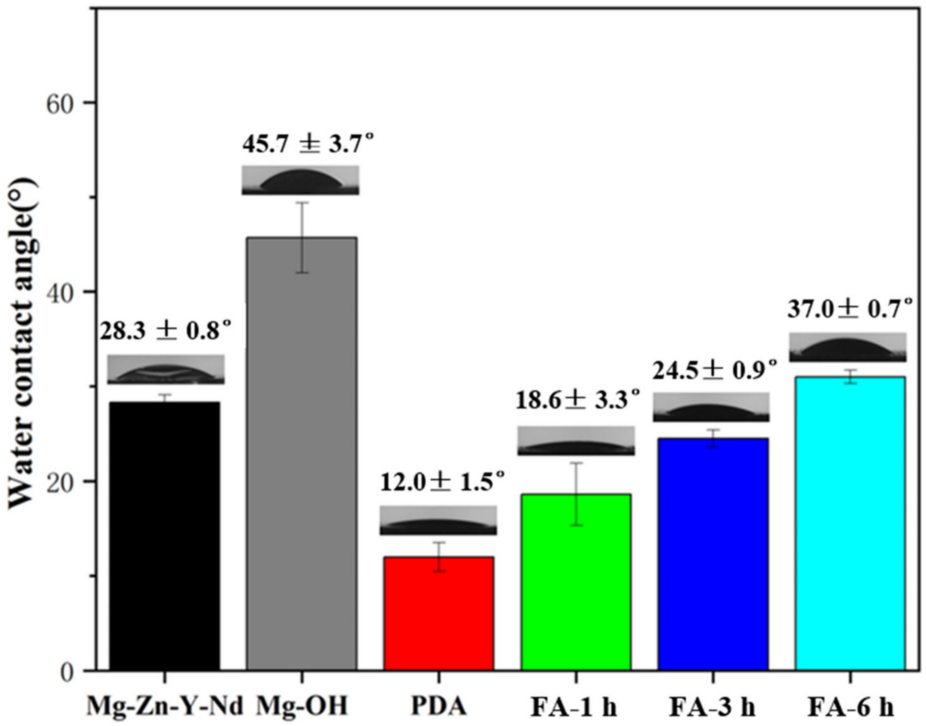

Figure 6. Water contact angle of samples (mean ± SD, n = 6).

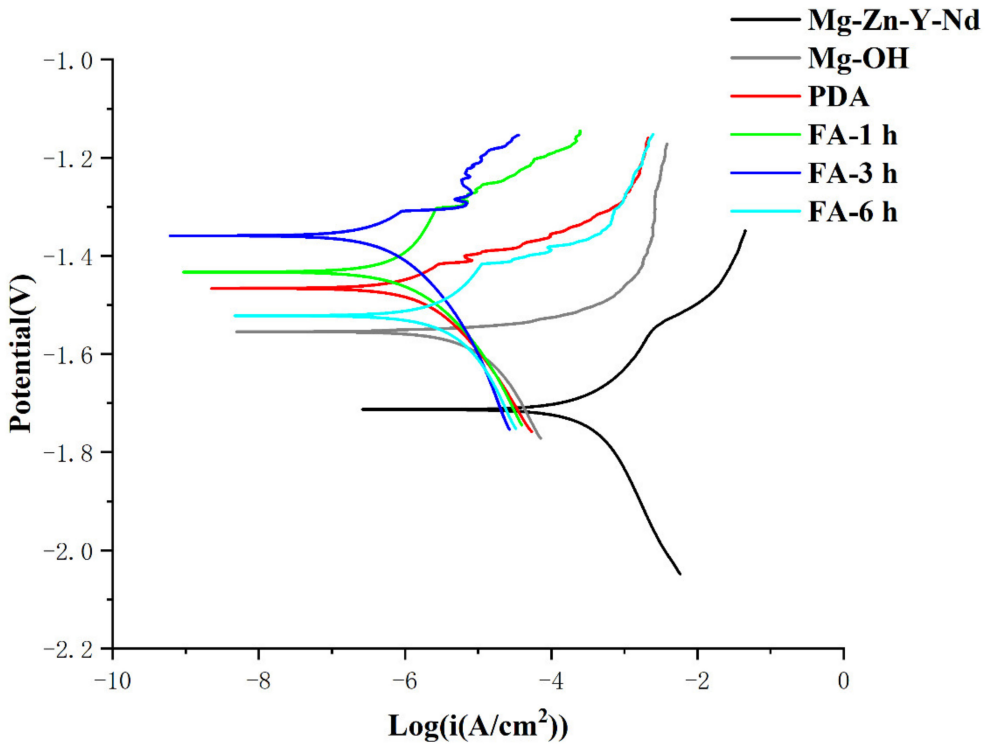

Figure 7. Potentiodynamic polarization plots of samples.

Table 1. Corrosion potential (Ecorr) and current density (Icorr) of samples.

Samples	E_{corr} (V)	I_{corr} (A/cm^2)
Mg-Zn-Y-Nd	−1.71	1.08×10^{-4}
Mg-OH	−1.55	2.47×10^{-6}
PDA	−1.47	6.50×10^{-7}
FA-1 h	−1.43	3.44×10^{-7}
FA-3 h	−1.36	2.06×10^{-7}
FA-6 h	−1.52	1.24×10^{-6}

In the low-frequency region, the intersection of the real part of the impedance and the x-axis reflected the impedance value of the sample. As shown in Figure 8, it can be found from the figure that the impedance value of Mg-Zn-Y-Nd was low, which was 129 Ohm, while the impedance values of Mg-OH and PDA samples were close, which were 5580 and 7080 Ohm, respectively. Moreover, the impedance of Fa-1 h, Fa-3 h, and Fa-6 h were 10,300, 10,900, and 12,200 Ohm, which was greater than that of the PDA coating and alkaline thermal coating, indicating that PDA/FA coating increased the corrosion resistance of the Mg alloy. The order of impedance was Fa-6 h > Fa-3 h > Fa-1 h > PDA > Mg-OH > Mg-Zn-Y-Nd. It is worth noting that the Fa-6 h impedance radius was larger, indicating good corrosion resistance, which may be due to slow corrosion in steady state.

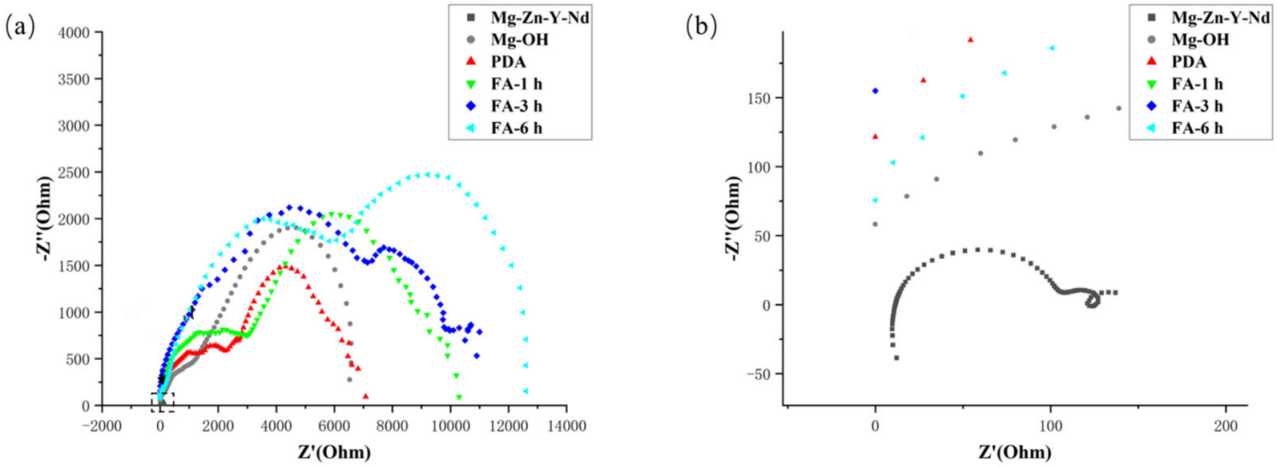

Figure 8. (**a**) EIS Nyquist spectra of the samples in the SBF solution; (**b**) EIS Nyquist spectra of Mg-Zn-Y-Nd in SBF solution.

3.3. Blood Compatibility Tests

As shown in Figure 9, the hemolysis rate of each sample was less than 5%, indicating that no hemolysis occurred. The order of hemolysis rate from largest to smallest was Mg-OH > Mg-Zn-Y-Nd > Fa-6 h > PDA > Fa-1 h > Fa-3 h. After FA was fixed, the hemolysis rate of the sample decreased. Although hydrothermal treatment improved the corrosion resistance of the Mg-Zn-Y-Nd alloy (Figures 7 and 8, Table 1), its hemolysis rate also further increased. FA coating can obviously significantly reduce the hemolysis rate of Mg-OH samples, but with the extension of coating preparation time, the hemolysis rate of samples may have the risk of rebound.

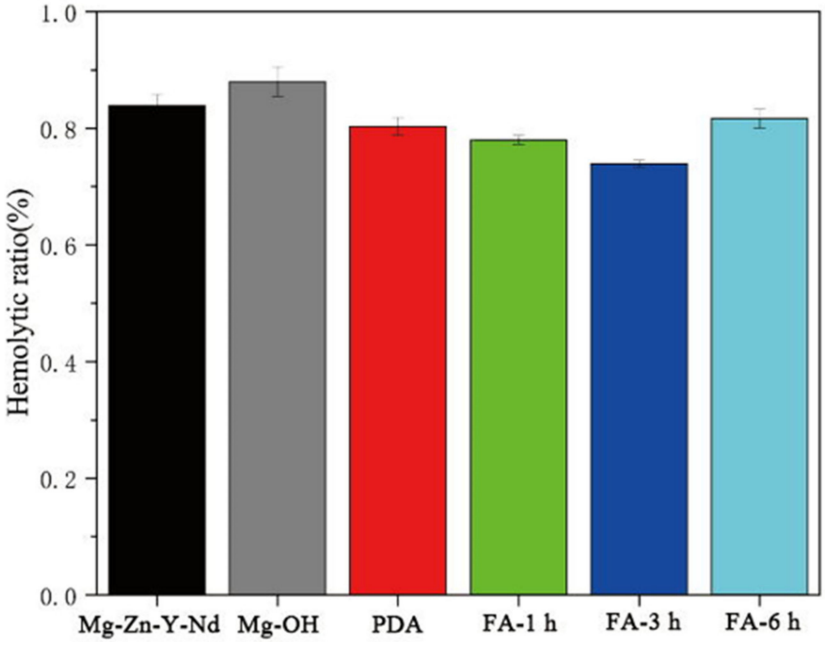

Figure 9. Hemolysis rate of each sample (mean ± SD, n = 3).

As shown in Figure 10, the numbers of adhesion and denaturation of fibrinogen (FGN) on the Mg alloy and alkali heat sample were larger, and the numbers of adhesion and denaturation of FGN after fixing FA were greatly reduced. The order of FGN adhesion from largest to smallest was Mg-OH > Mg-Zn-Y-Nd > Fa-1 h > Fa-3 h > Fa-6 h > PDA. The order of FGN denaturation quantity from largest to smallest is Mg-Zn-Y-Nd > Mg-OH > Fa-6 h > PDA > Fa-3 h > Fa-1 h. This indicated that PDA/FA coating can inhibit the adhesion and denaturation of FGN.

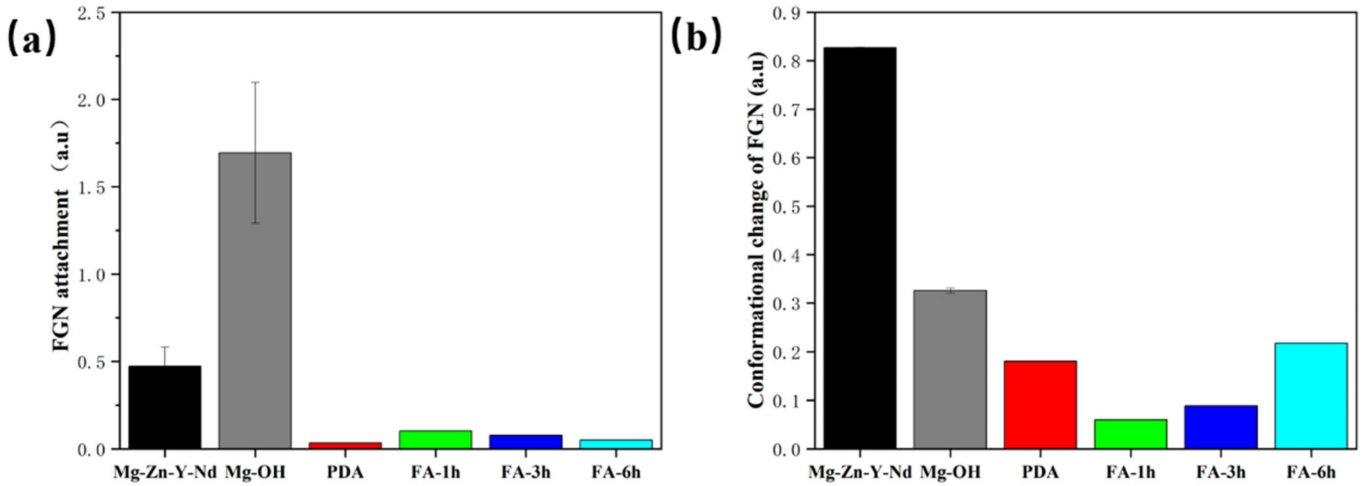

Figure 10. Adhesion (**a**) and denaturation (**b**) of FGN in each sample (mean ± SD, n = 3).

Research shows that Mg alloys have poor blood compatibility due to rapid degradation [43]. As shown in Figure 11, consistent with the literature, the Mg alloy was corroded, and a large number of platelets gathered on the surface, indicating that the Mg alloy may induce platelet activation. On the PDA coating, the platelets were partially aggregated, interconnected, and they extended pseudopodia showing a flat shape and a fully activated state, which indicated that the anti-platelet aggregation ability of PDA coating was poor. This may be because the PDA coating has good hydrophilicity and contains a large number of positive charges, which will adsorb negatively charged platelets and fibrin. After FA

fixation, the number of platelets decreased significantly at 1 h, and some showed a spiny structure and tended to be activated. At 3 h, platelets were not spherical and showed an inactive state. At 6 h, the whole platelet still showed a spherical inactive state, but some platelets protrude pseudopodia. This indicates that FA may have good and obvious anti-platelet adhesion ability by inhibiting FGN adhesion and degeneration, or that FA inhibits platelet activity by antagonizing thromboxane.

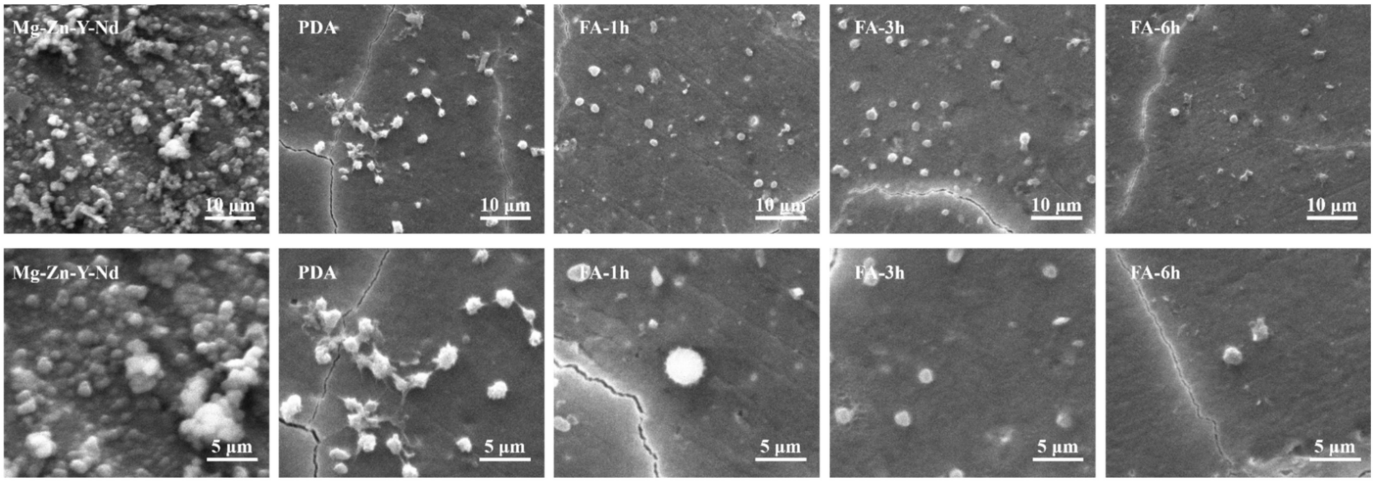

Figure 11. Platelet adhesion morphology of each sample.

The grafting time of FA corresponds to its amount on the surface. Generally, more molecules will be fixed on the surface after a longer grafting time, but this does not mean that a coating composed of more molecules will possess better functions [34]. In this study, the FA-6 h samples showed fewer platelets compared with FA-1 h and FA-3 h, but higher FGN denaturation compared to FA-1 h and FA-3 h. The platelet activation of FA-6 h was also more severe than FA-3 h. The reason may be due to its excessive preparation time. The weaker corrosion resistance of FA-6 h compared to that of FA-1 h and FA-3 h in Figure 7 and in Table 1 also indicated that its degradation behavior also affected blood compatibility.

3.4. DPPH Free Radical Content Test

The DPPH method was used to evaluate its free radical scavenging ability (Figure 12). The content of free radicals in the blank control group was the highest, and the content of free radicals decreased after adding the sample. The order of free radical scavenging ability was Fa-1 h > Fa-3 h > Fa-6 h > Mg-Zn-Y-Nd > PDA. The DPPH experiment showed that compared with the Mg alloy and PDA coating, FA fixation could significantly improve the free radical scavenging ability of the sample. The data of scavenging free radicals show that FA fixation can significantly improve the antioxidant capacity of the Mg alloy and PDA coating, which means that the coating can provide a good environment for the adhesion and proliferation of endothelial cells.

An ideal Mg alloy cardiovascular stent needs to reduce the adsorption of fibrin, promote the adhesion and proliferation of endothelial cells, inhibit the adhesion and proliferation of smooth muscle cells, and provide a good microenvironment for the implantation of cardiovascular stents. Therefore, surface modification and loading of new drugs is very important, and ferulic acid has the above functions. In this work, we used ferulic acid, a cardiovascular drug and antioxidant, as well as an extract of traditional Chinese medicine, combined with polydopamine to obtain a uniform and dense coating. After preparation, the coating has good oxidation resistance, which provides a new solution for the surface modification of Mg alloy cardiovascular stents.

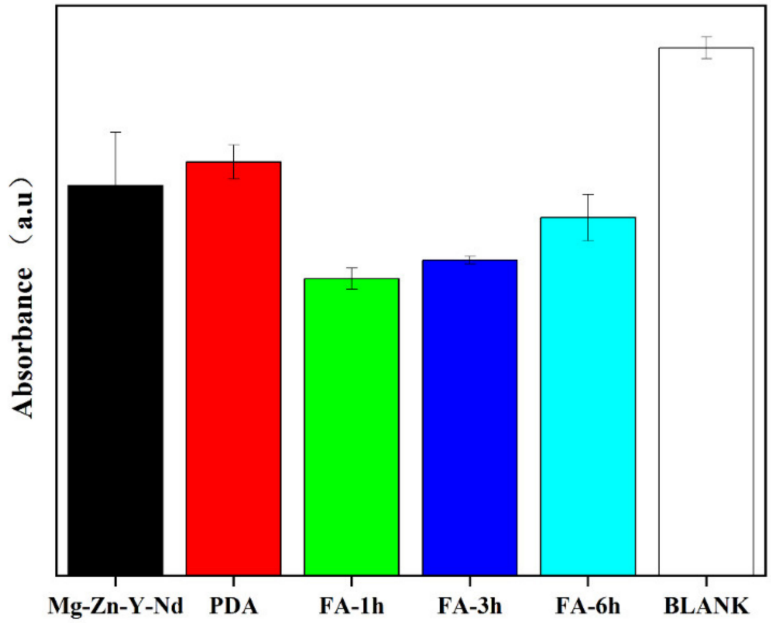

Figure 12. DPPH radical content of samples.

4. Conclusions

In this paper, the surface of Mg-Zn-Y-Nd alloy was modified by preparing a PDA/FA functional coating, which improved the corrosion resistance and biocompatibility of an Mg alloy. The modification of uniform PDA/FA coating makes the Mg alloy have better corrosion resistance, improves the anticoagulant ability, and widens the application of Mg alloy. It is worth noting that Fa-3 h has good corrosion resistance and blood compatibility. In summary, a functional composite coating is studied, which provides a new idea for the application of the medical Mg alloy.

Author Contributions: Conceptualization, Z.H. and Y.Z.; methodology, Z.H. and H.G.; software, Z.H. and H.G.; validation, Y.Z. and J.-a.L.; formal analysis, Z.H.; investigation, Z.H.; resources, Y.Z.; data curation, Y.Z.; writing—original draft preparation, Z.H.; writing—review and editing, J.-a.L. and Y.Z.; visualization, Y.Z.; supervision, L.W.; funding acquisition, Y.Z., K.Z. and J.-a.L. All authors have read and agreed to the published version of the manuscript.

Funding: This research was funded by National Nature Science Foundation of China (No. U2004164 and 51671175).

Institutional Review Board Statement: Not applicable.

Informed Consent Statement: Not applicable.

Data Availability Statement: The data presented in this study are available on request from the authors.

Conflicts of Interest: The authors declare no conflict of interest.

References

1. Roth, G.A.; Johnson, C.; Abajobir, A.; Abd-Allah, F.; Abera, S.F.; Abyu, G.; Ahmed, M.; Aksut, B.; Alam, T.; Alam, K.; et al. Regional, and National Burden of Cardiovascular Diseases for 10 Causes, 1990 to 2015. *J. Am. Coll. Cardiol.* **2017**, *70*, 1–25. [CrossRef] [PubMed]
2. Li, J. Advanced Biomaterials for Drug Delivery and Tissue Regeneration. *Curr. Drug Deliv.* **2021**, *18*, 834–835. [CrossRef] [PubMed]
3. Crimi, G.; Gritti, V.; Galiffa, V.A.; Scotti, V.; Leonardi, S.; Ferrario, M.; Ferlini, M.; De Ferrari, G.M.; Visconti, L.O.; Klersy, C. Drug eluting stents are superior to bare metal stents to reduce clinical outcome and stent-related complications in CKD patients, a systematic review, meta-analysis and network meta-analysis. *J. Interv. Cardiol.* **2018**, *31*, 319–329. [CrossRef] [PubMed]
4. Wei, S.; Xu, Y.; Wang, Z.; Li, M.; Sun, P.; Xie, B.; Xing, Y.; Bai, H.; Kan, Q.; Li, J.; et al. Hydrogel-coated needles prevent puncture site bleeding. *Acta Biomater.* **2021**, *128*, 305–313. [CrossRef] [PubMed]

5. Iakovou, I.; Schmidt, T.; Bonizzoni, E.; Ge, L.; Sangiorgi, G.M.; Stankovic, G.; Airoldi, F.; Chieffo, A.; Montorfano, M.; Carlino, M.; et al. Incidence, Predictors, and Outcome of Thrombosis After Successful Implantation of Drug-Eluting Stents. *JAMA* **2005**, *293*, 2126–2130. [CrossRef]
6. Yu, Y.; Zhu, S.; Hou, Y.; Li, J.; Guan, S. Sulfur contents in sulfonated hyaluronic acid direct the cardiovascular cells fate. *ACS Appl. Mater. Interfaces* **2020**, *12*, 46827–46836. [CrossRef]
7. Sketch, M.H.; Ball, M.; Rutherford, B.; Popma, J.J.; Russell, C.; Kereiakes, D.J.; on behalf of the Driver Investigators. Evaluation of the Medtronic (Driver) cobalt-chromium alloy coronary stent system. *Am. J. Cardiol.* **2005**, *95*, 8–12. [CrossRef]
8. Dong, H.; Li, D.; Mao, D.; Bai, N.; Chen, Y.; Li, Q. Enhanced performance of magnesium alloy for drug-eluting vascular scaffold application. *Appl. Surf. Sci.* **2018**, *435*, 320–328. [CrossRef]
9. Hou, Y.; Witte, F.; Li, J.; Guan, S. The increased ratio of Mg^{2+}/Ca^{2+} from degrading magnesium alloys directs macrophage fate for functionalized growth of endothelial cells. *Smart Mater. Med.* **2022**, *3*, 188–198. [CrossRef]
10. Witte, F.; Hort, N.; Vogt, C.; Cohen, S.; Kainer, K.U.; Willumeit, R.; Feyerabend, F. Degradable biomaterials based on magnesium corrosion. *Curr. Opin. Solid State Mater. Sci.* **2008**, *12*, 63–72. [CrossRef]
11. Liu, C.; Hou, Y.; Li, J. A mini review on biodegradable magnesium alloy vascular stent. *Adv. Mater. Lett.* **2020**, *11*, 20101563. [CrossRef]
12. Zhao, Z.; Moghadasian, M.H. Chemistry, natural sources, dietary intake and pharmacokinetic properties of ferulic acid: A review. *Food Chem.* **2008**, *109*, 691–702. [CrossRef] [PubMed]
13. Kumar, N.; Pruthi, V. Potential applications of ferulic acid from natural sources. *Biotechnol. Rep.* **2014**, *4*, 86–93. [CrossRef] [PubMed]
14. Sanduk, F.; Meng, Y.; Widera, D.; Kowalczyk, R.M.; Michael, N.; Kaur, A.; Yip, V.; Zulu, S.; Zavrou, I.; Hana, L.; et al. Enhanced anti-inflammatory potential of degradation resistant curcumin/ferulic acid eutectics embedded in triglyceride-based microemulsions. *J. Drug Deliv. Sci. Technol.* **2020**, *60*, 102067. [CrossRef]
15. Wang, B.H.; Ou-Yang, J.P. Pharmacological Actions of Sodium Ferulate in Cardiovascular System. *Cardiovasc. Drug Rev.* **2010**, *23*, 161–172. [CrossRef]
16. Lin, C.M.; Chiu, J.H.; Wu, I.H.; Wang, B.W.; Pan, C.M.; Chen, Y.H. Ferulic acid augments angiogenesis via VEGF, PDGF and HIF-1 alpha. *J. Nutr. Biochem.* **2010**, *21*, 627–633. [CrossRef]
17. Wang, J.; Yuan, Z.; Zhao, H.; Ju, D.; Chen, Y.; Chen, X.; Zhang, J. Ferulic acid promotes endothelial cells proliferation through up-regulating cyclin D1 and VEGF. *J. Ethnopharmacol.* **2011**, *137*, 992–997. [CrossRef]
18. Hou, Y.Z.; Yang, J.; Zhao, G.R.; Yuan, Y.J. Ferulic acid inhibits vascular smooth muscle cell proliferation induced by angiotensin II. *Eur. J. Pharmacol.* **2004**, *499*, 85–90. [CrossRef]
19. Zhang, E.; Shen, F. Blood compatibility of a ferulic acid (FA)-eluting PHBHHx system for biodegradable magnesium stent application. *Mater. Sci. Eng. C Mater. Biol. Appl.* **2015**, *52*, 37–45. [CrossRef]
20. Li, J.; Chen, L.; Zhang, X.; Guan, S. Enhancing biocompatibility and corrosion resistance of biodegradable Mg-Zn-Y-Nd alloy by preparing PDA/HA coating for potential application of cardiovascular biomaterials. *Mater. Sci. Eng. C* **2020**, *109*, 110607. [CrossRef]
21. Liang, J.; Cui, L.; Li, J.K.; Guan, S.; Zhang, K.; Li, J. Aloe vera: A medicinal plant used in skin wound healing. *Tissue Eng. Part B Rev.* **2021**, *27*, 455–474. [CrossRef] [PubMed]
22. Wei, S.; Li, J.; He, H.; Shu, C.; Dardik, A.; Bai, H. A three-layered hydrogel patch with hierarchy releasing of PLGA nanoparti-cle drugs decrease neointimal hyperplasia. *Smart Mater. Med.* **2022**, *3*, 139–147. [CrossRef]
23. Ho, C.C.; Ding, S.J. Structure, properties and applications of mussel-inspired polydopamine. *J. Biomed. Nanotechnol.* **2014**, *10*, 3063–3084. [CrossRef] [PubMed]
24. Chen, D.; Wang, R.; Huang, Z.; Wu, Y.; Zhang, Y.; Wu, G.; Li, D.; Guo, C.; Jiang, G.; Yu, S.; et al. Evolution processes of the corrosion behavior and structural characteristics of plasma electrolytic oxidation coatings on AZ31 magnesium alloy. *Appl. Surf. Sci.* **2018**, *434*, 326–335. [CrossRef]
25. Liu, X.; Zhen, Z.; Liu, J.; Xi, T.; Zheng, Y.; Guan, S.; Zheng, Y.; Cheng, Y. Multifunctional MgF_2/Polydopamine Coating on Mg Alloy for Vascular Stent Application. *J. Mater. Sci. Technol.* **2015**, *31*, 733–743. [CrossRef]
26. Tong, P.; Sheng, Y.; Hou, R.; Iqbal, M.; Chen, L.; Li, J. Recent progress on coatings of biomedical magnesium alloy. *Smart Mater. Med.* **2022**, *3*, 104–116. [CrossRef]
27. Yang, Y.X.; Fang, Z.; Liu, Y.H.; Hou, Y.C.; Wang, L.G.; Zhou, Y.F.; Zhu, S.J.; Zeng, R.C.; Zheng, Y.F.; Guan, S.K. Biodegradation, hemocompatibility and covalent bonding mechanism of electrografting polyethylacrylate coating on Mg alloy for cardiovascular stent. *J. Mater. Sci. Technol.* **2020**, *46*, 114–126. [CrossRef]
28. Huang, W.; Mei, D.; Liu, Y.; Wang, L.; Zhou, Y.; Zhu, S.; Guan, S. A simple approach for synthesizing polyglycolide coating on magnesium alloy. *Mater. Lett.* **2021**, *298*, 130046. [CrossRef]
29. Liu, J.; Zheng, B.; Wang, P.; Wang, X.; Zhang, B.; Shi, Q.; Xi, T.; Chen, M.; Guan, S. Enhanced in Vitro and in Vivo Performance of Mg-Zn-Y-Nd Alloy Achieved with APTES Pretreatment for Drug-Eluting Vascular Stent Application. *ACS Appl. Mater. Interfaces* **2016**, *8*, 17842–17858. [CrossRef]
30. Liu, J.; Xi, T. Enhanced Anti-corrosion Ability and Biocompatibility of PLGA Coatings on MgZnYNd Alloy by BTSE-APTES Pre-treatment for Cardiovascular Stent. *J. Mater. Sci. Technol.* **2016**, *32*, 845–857. [CrossRef]

31. Sheng, Y.; Yang, J.; Hou, R.; Chen, L.; Xu, J.; Liu, H.; Zhao, X.; Wang, X.; Zeng, R.; Li, W.; et al. Improved biocompatibility and degradation behavior of biodegradable Zn-1Mg by grafting zwitterionic phosphorylcholine chitosan (PCCs) coating on silane pre-modified surface. *Appl. Surf. Sci.* **2020**, *527*, 146914. [CrossRef]
32. Chen, Y.; Wan, G.; Wang, J.; Zhao, S.; Zhao, Y.; Huang, N. Covalent immobilization of phytic acid on Mg by alkaline pre-treatment: Corrosion and degradation behavior in phosphate buffered saline. *Corros. Sci.* **2013**, *75*, 280–286. [CrossRef]
33. Yang, Z.; Xiong, K.; Qi, P.; Yang, Y.; Tu, Q.; Wang, J.; Huang, N. Gallic acid tailoring surface functionalities of plasma-polymerized allylamine-coated 316L SS to selectively direct vascular endothelial and smooth muscle cell fate for enhanced endothelialization. *ACS Appl. Mater. Interfaces* **2014**, *6*, 2647–2656. [CrossRef]
34. Chen, L.; Li, J.; Chang, J.; Jin, S.; Wu, D.; Yan, H.; Wang, X.; Guan, S. Mg-Zn-Y-Nd coated with citric acid and dopamine by layer-by-layer self-assembly to improve surface biocompatibility. *Sci. China Technol. Sci.* **2018**, *61*, 1228–1237. [CrossRef]
35. Li, J.; Li, W.; Zou, D.; Kou, F.; Hou, Y.; Yasin, A.; Zhang, K. Comparison of conjugating chondroitin sulfate A and B on amine-rich surface: For deeper understanding on directing cardiovascular cells fate. *Compos. Part B Eng.* **2022**, *228*, 109430. [CrossRef]
36. Bai, H.; Sun, P.; Wu, H.; Wei, S.; Xie, B.; Wang, W.; Hou, Y.; Li, J.; Dardik, A.; Li, Z. The application of tissue-engineered fish swim bladder vascular graft. *Commun. Biol.* **2021**, *4*, 1153. [CrossRef] [PubMed]
37. Yu, Y.; Zhu, S.J.; Dong, H.T.; Zhang, X.Q.; Li, J.A.; Guan, S.K. A novel MgF_2/PDA/S-HA coating on the biodegradable ZE21B alloy for better multi-functions on cardiovascular application. *J. Magnes. Alloys* **2021**. [CrossRef]
38. Zou, D.; Li, J.; Kou, F.; Luo, X.; Yang, P. Reveal crucial subtype of natural chondroitin sulfate on the functionalized coatings for cardiovascular implants. *J. Mater. Sci. Technol.* **2021**, *91*, 67–77. [CrossRef]
39. Li, J.; Wang, S.; Sheng, Y.; Liu, C.; Xue, Z.; Tong, P.; Guan, S. Designing HA/PEI nanoparticle composite coating on biodegradable Mg-Zn-Y-Nd alloy to direct cardiovascular cells fate. *Smart Mater. Med.* **2021**, *2*, 124–136. [CrossRef]
40. Kou, F.; Liu, C.; Wang, L.; Yasin, A.; Li, J.; Guan, S. Fabrication of Citric Acid/RGD Multilayers on Mg-Zn-Y-Nd Alloy via Layer-by-Layer Self-Assembly for Promoting Surface Biocompatibility. *Adv. Mater. Interfaces* **2021**, *8*, 2002241. [CrossRef]
41. Wu, Y.; Chang, L.; Li, J.; Wang, L.; Guan, S. Conjugating heparin, REDV peptide and anti-CD34 to the silanic Mg-Zn-Y-Nd alloy for better endothelialization. *J. Biomater. Appl.* **2020**, *35*, 158–168. [CrossRef] [PubMed]
42. Xu, R.; Zhang, K.; Liang, J.; Gao, F.; Li, J.; Guan, F. Hyaluronic acid/polyethyleneimine nanoparticles loaded with copper ion and disulfiram for esophageal cancer. *Carbohydr. Polym.* **2021**, *261*, 117846. [CrossRef] [PubMed]
43. Wei, Z.; Tian, P.; Liu, X.; Zhou, B. In vitro degradation, hemolysis, and cytocompatibility of PEO/PLLA composite coating on biodegradable AZ31 alloy. *J. Biomed. Mater. Res. Part B* **2015**, *103B*, 342–354. [CrossRef] [PubMed]